

**SUPPLEMENTAL INFORMATION TO:**

**“LKB1/STK11 Inactivation Leads to Expansion of A Pro-Metastatic Tumor Sub-Population in Melanoma” (MS # 11-00619):**

**Inventory of supplemental information**

Table S1, related to Figure 2

Table S2, related to Figure 6

Table S3, related to Figure 6

Movie S1, related to Figure 3

Movie S2, related to Figure 3

Figure S1, related to Figure 1

Figure S2, related to Figure 2

Figure S3, related to Figure 3

Figure S4, related to Figure 4

Figure S5, related to Figure 5

Figure S6, related to Figure 6

Figure S7, related to Figure 7

Figure S8, related to Figure 8

**DESCRIPTION OF TABLES:**

**Table S1, Tumor formation and metastasis by genotype and site in GEM models of melanoma, related to Figure 2.**

Genotype	Primary Tumors/Treated Mice	# Metastases by Site					
		L.N.	Lung	Liver	Spleen	Kidney	Brain
<i>TK</i>	0/12	0	0	0	0	0	0
<i>TKp16<sup>L/L</sup></i>	8/11	0	0	0	0	0	0
<i>TKp53<sup>L/L</sup></i>	8/11	0	0	0	0	0	0
<i>TKp53<sup>L/L</sup>p16<sup>L/L</sup></i>	15/15	0	0	0	0	0	0
<i>TKLkb1<sup>L/L</sup></i>	12/12	12	2	2	3	0	0
<i>TKp53<sup>L/L</sup>Lkb1<sup>L/L</sup></i>	15/15	15	5	3	4	0	0

*TK*=*Tyr-CRE-ER<sup>T2</sup> Kras<sup>LSL/+</sup>*; L.N. = lymph node.

**Table S2, Transcripts associated with Lkb1 status in cell lines and primary tumors (FDR<0.05), related to Figure 6.**

**Table S3, Gene set enrichment analysis (GSEA) of the overlapping genes in both tumor and cell line samples, related to Figure 6. Data Attached.**

## DESCRIPTION OF MOVIES:

**Movie S1, related to Figure 3.** *TKLkb1<sup>L/L</sup>* cells were visualized in the scratch assay for 12 hours after wounding. Images were taken every 30 minutes. Original mag. = 4x.

**Movie S2, related to Figure 3.** *TKp53<sup>L/L</sup>p16<sup>L/L</sup>* cells were visualized in the scratch assay for 12 hours after wounding. Images were taken every 30 minutes. Original mag. = 4x.

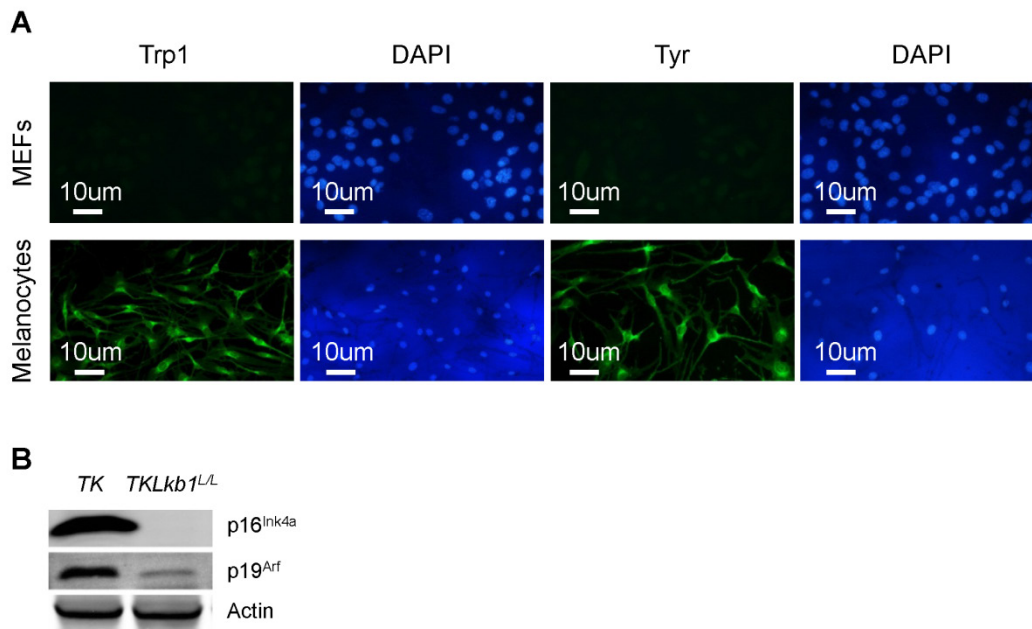


**Figure S1, *In vitro* culture of primary melanocytes, related to Figure 1.** (A) Primary melanocytes were subjected to immunofluorescence staining for the expression of tyrosinase-related protein 1 (Trp1) and tyrosinase (Tyr). Murine Embryo Fibroblasts were included as a control. (B) Representative western analysis of *TK* and *TKLkb1<sup>L/L</sup>* melanocytes after 50 days of *in vitro* culture.

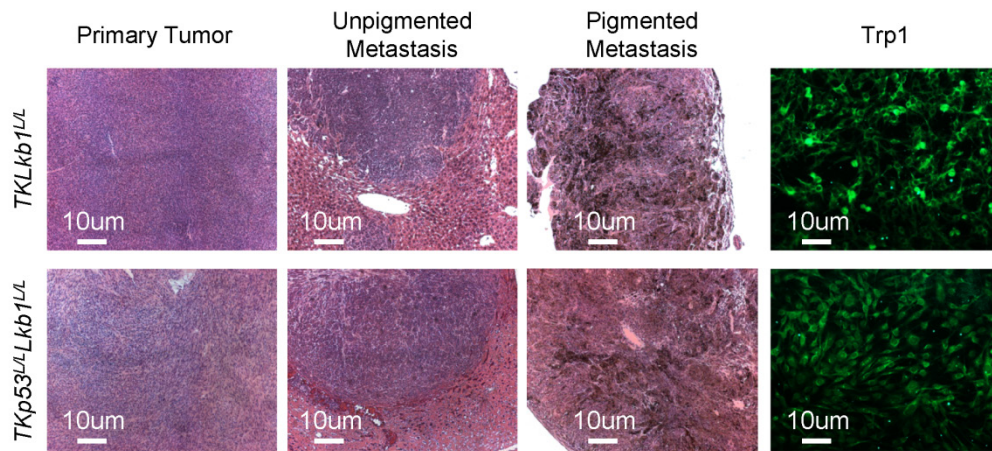


**Figure S2, Histological analysis of *Lkb1*-null tumors, related to Figure 2.** H&E staining was performed on tumor tissues of indicated genotypes. Immunofluorescence staining for the expression of Trp1 was performed on cells cultured from tumors.

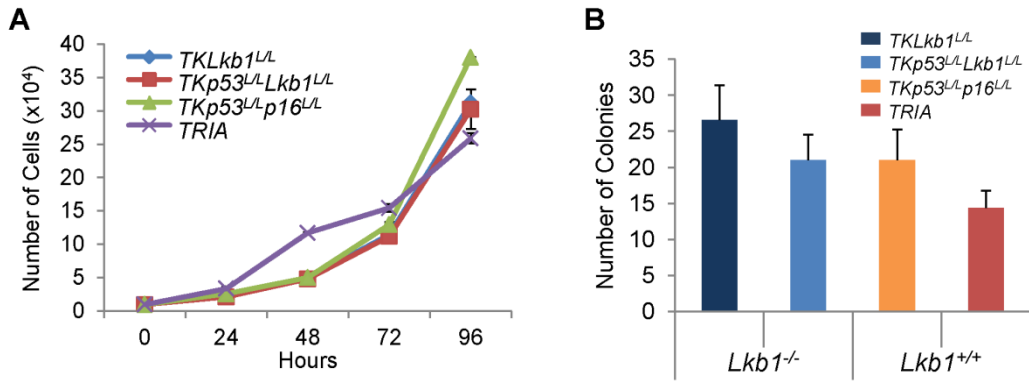


**Figure S3, Growth curves and anchorage-independent growth in soft agar, related to Figure 3.** (A) Growth curves of indicated *Lkb1*-deficient (*TKLkb1<sup>L/L</sup>* and *TKp53<sup>L/L</sup>Lkb1<sup>L/L</sup>*) and *Lkb1*-competent (*TKp53<sup>L/L</sup>p16<sup>L/L</sup>* and *TRIA*) melanoma cells. (B) Anchorage-independent growth of indicated tumor cells in soft agar. The number of colonies was quantified. Error bars show standard deviation.

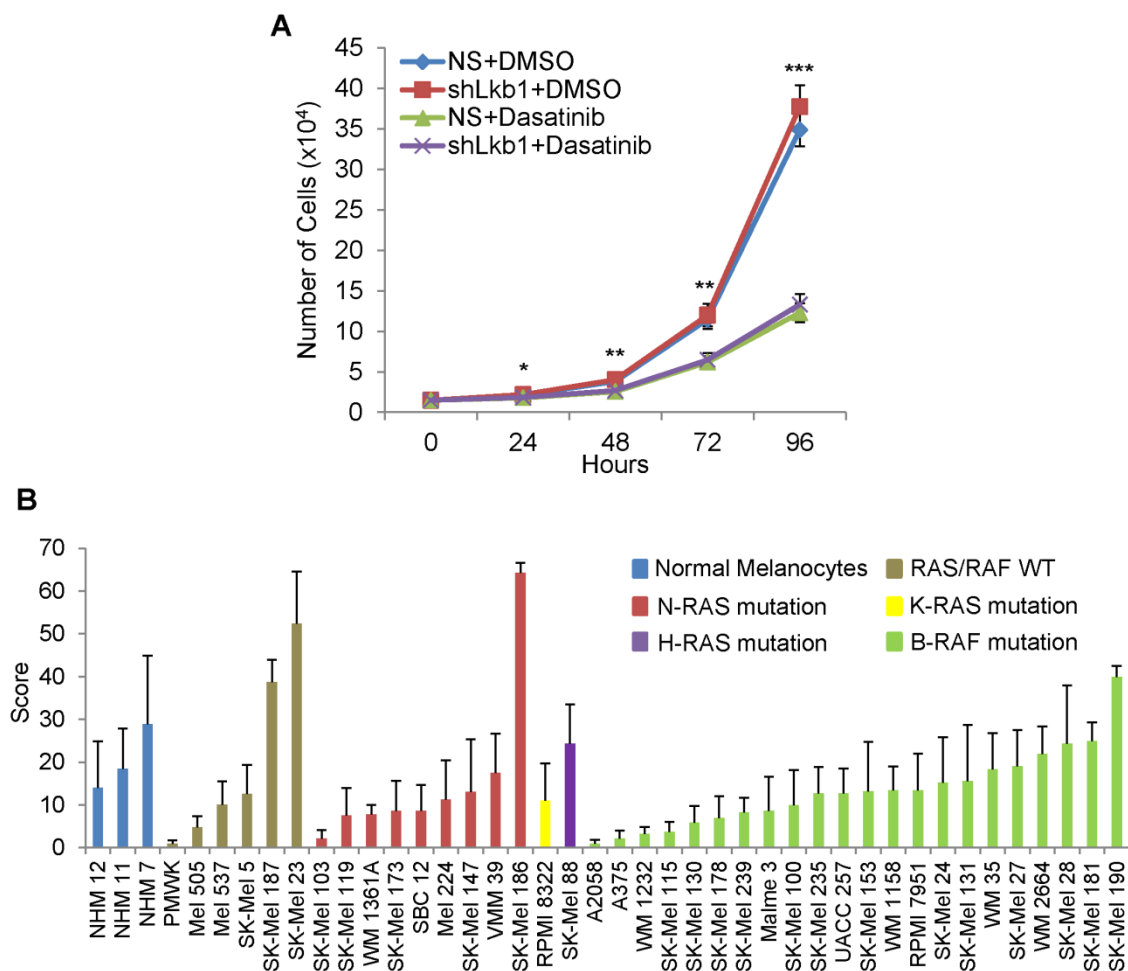


**Figure S4, The effects of dasatinib on cell growth and Cell Line Tissue Microarray analysis of LKB1 expression, related to Figure 4. (A)** Growth curves of *TKp53<sup>L/L</sup>p16<sup>L/L</sup>* cells with or without Lkb1 knockdown treated with vehicle (DMSO) or dasatinib (30 nM). Cell numbers were counted at indicated times. Error bars show standard deviation. \*:  $p < 0.05$ ; \*\*:  $p < 0.01$ ; \*\*\*:  $p < 0.001$ . **(B)** Cell Line Tissue Microarray (TMA) analysis of LKB1 expression. Expression of LKB1 was measured using Aperio V9 color deconvolution (area analysis). The color deconvolution algorithm score (0-300) output was used to estimate target protein expression. Cell lines are grouped by RAS and RAF mutation

status. Normal Human Melanocytes (NHM, in blue) are shown for comparison. Error bars represent standard error of the mean based on LKB1 quantification in at least three independent cores of each cell line.



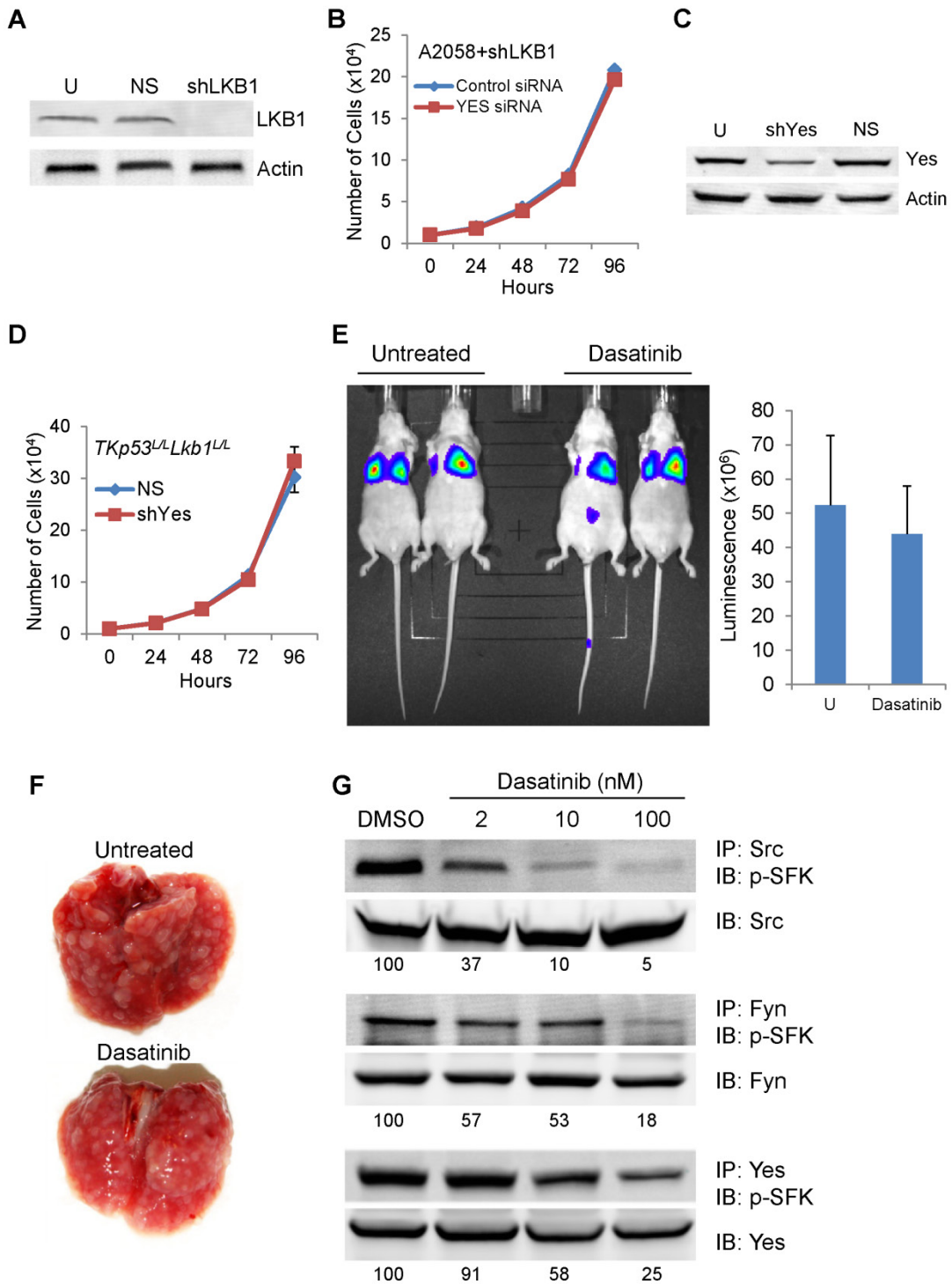


**Figure S5, The effects of Yes knockdown and dasatinib treatment, related to Figure 5.** (A) Representative western analysis of A2058 human melanoma cells transduced with nonspecific shRNA (NS) or shRNA to LKB1 (shLKB1). U: untreated. (B) Growth curves of A2058 cells transduced with scrambled control siRNAs or siRNAs targeting YES. (C) Representative western analysis of *TKp53<sup>L/L</sup>Lkb1<sup>L/L</sup>* melanoma cells transduced with nonspecific shRNA (NS) or shRNA to Yes (shYes). U: untreated. (D) *In vitro* growth curves of *TKp53<sup>L/L</sup>Lkb1<sup>L/L</sup>* melanoma cells transduced with nonspecific shRNA or shYes. (E-F) Luciferase-expressing *TKp53<sup>L/L</sup>Lkb1<sup>L/L</sup>* melanoma cells were injected into nude mice via tail vein and treated with or without dasatinib (50 mg/kg/day given orally). N=6 for each group. Three weeks after tail vein injection, mice were examined by luciferase imaging (E) and dissection (F). Luminescence was quantified. (G) *TKp53<sup>L/L</sup>Lkb1<sup>L/L</sup>* melanoma cells were treated with DMSO or increasing doses of dasatinib. Cell lysates were immunoprecipitated (IP) first with indicated antibodies against Src, Fyn or Yes, and then immunoblotted (IB) with antibody against p-SFKs (Y416). Relative phosphorylation levels with dasatinib treatment were quantified by LICOR and are shown at the bottom. Error bars show standard deviation in panels B, D, E.

A

Upregulated by Lkb1 loss

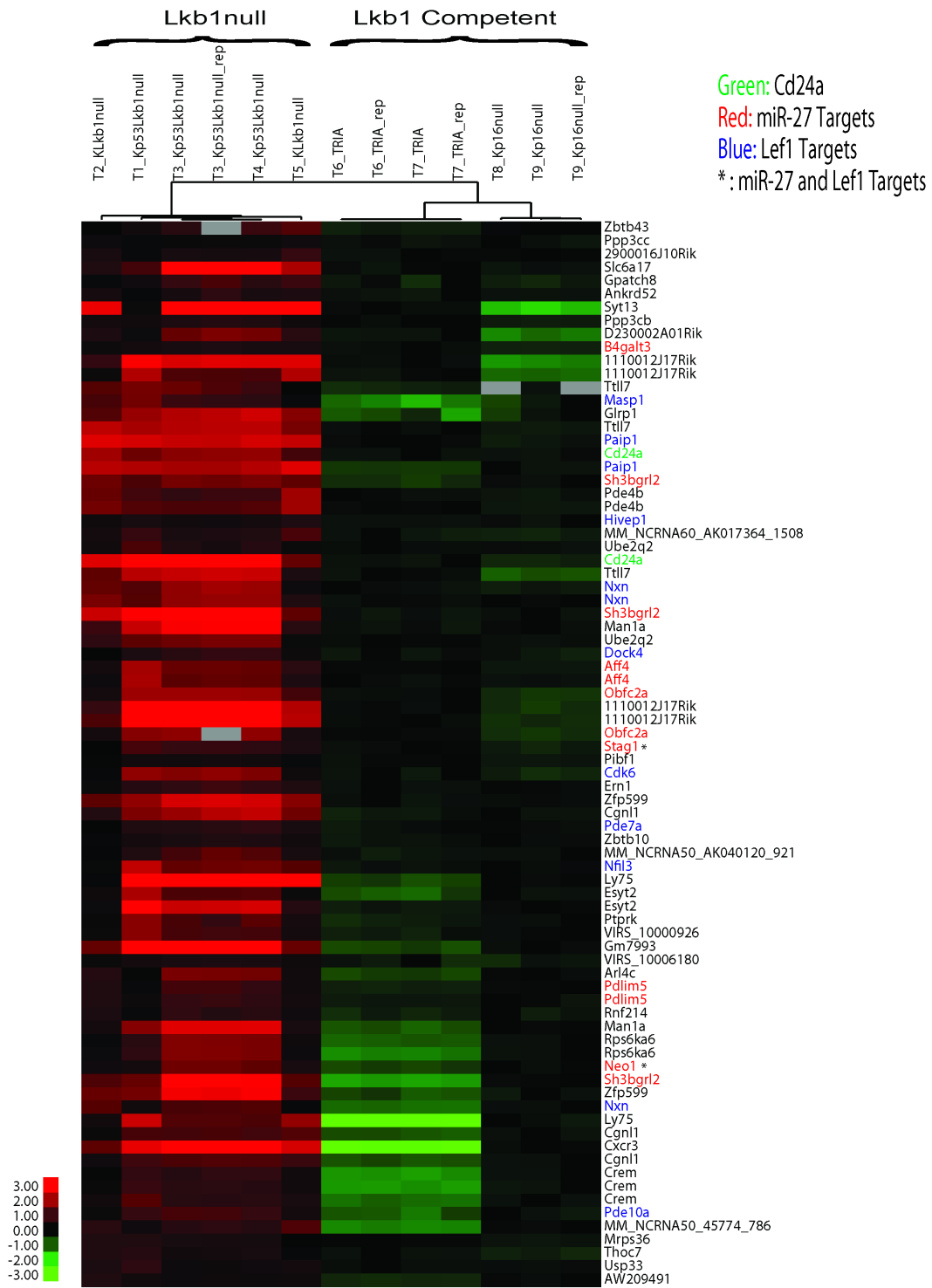


Figure S6, continued

**B**

Downregulated by Lkb1 loss

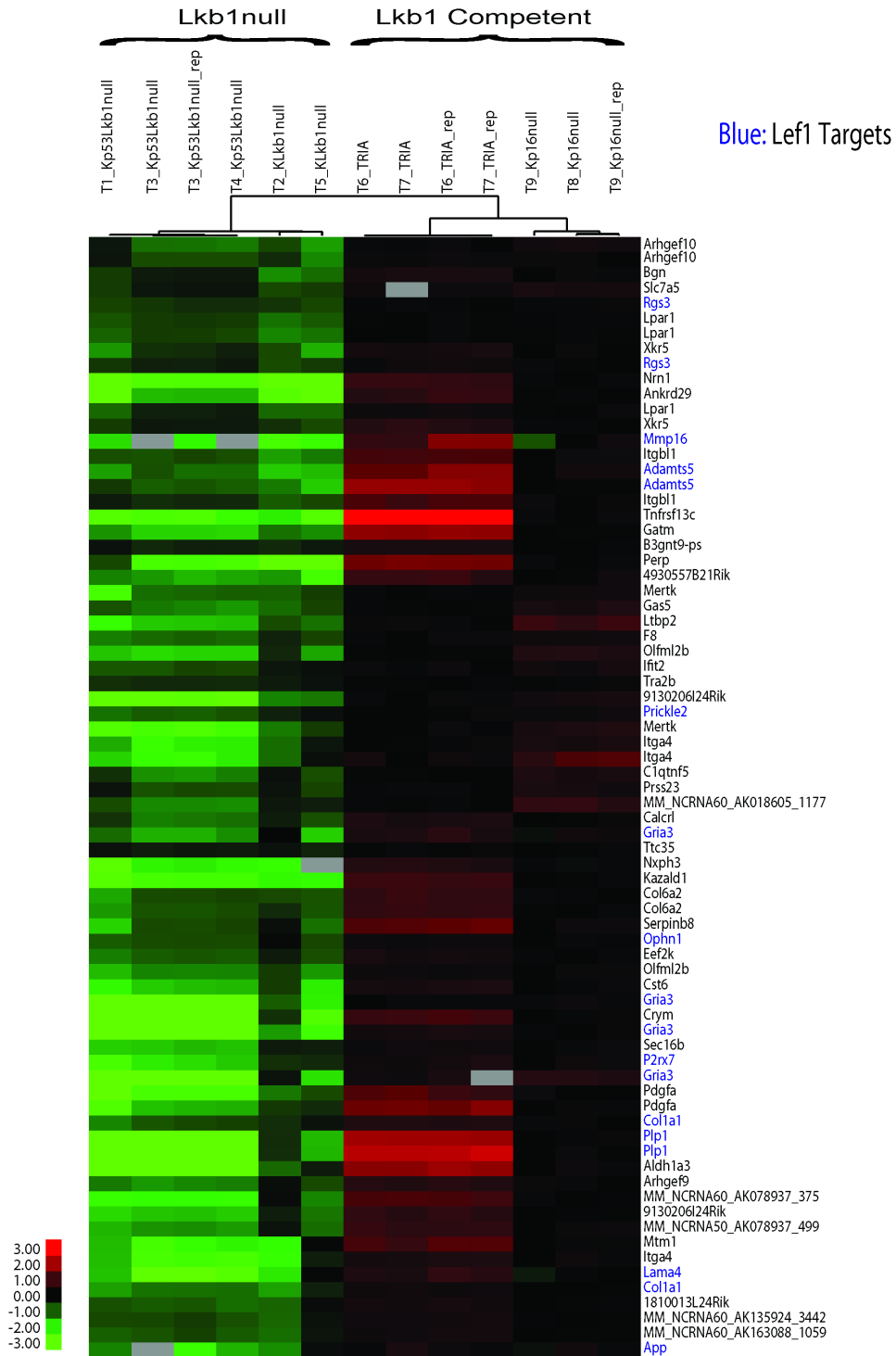


Figure S6, continued

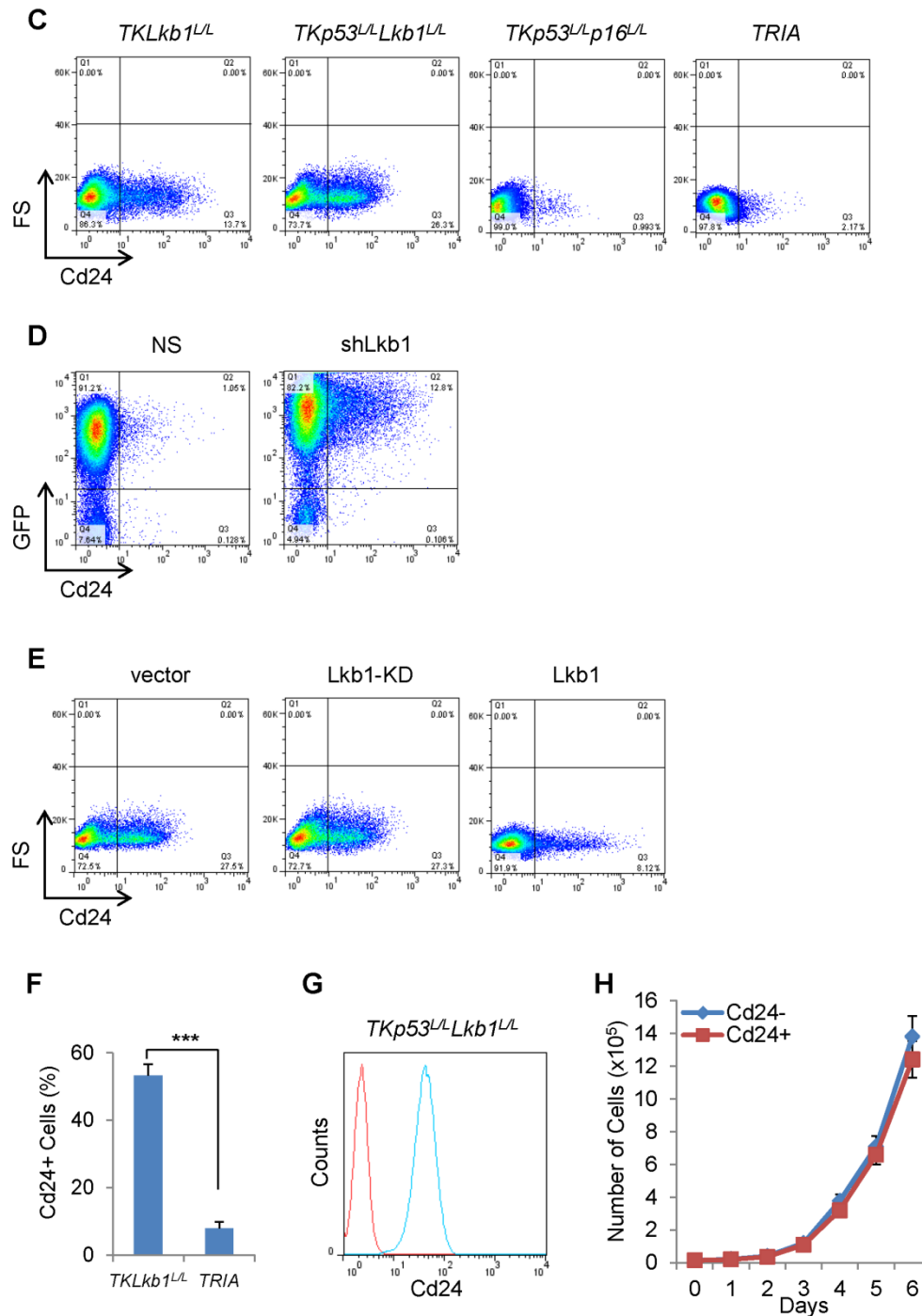
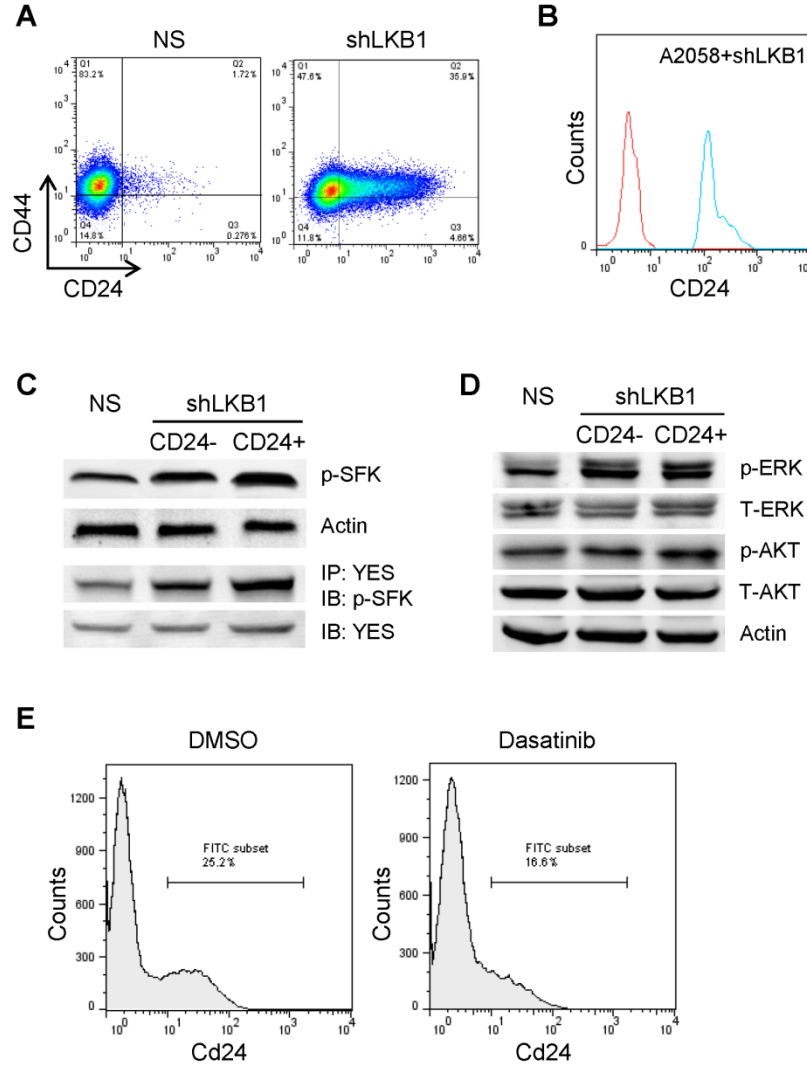
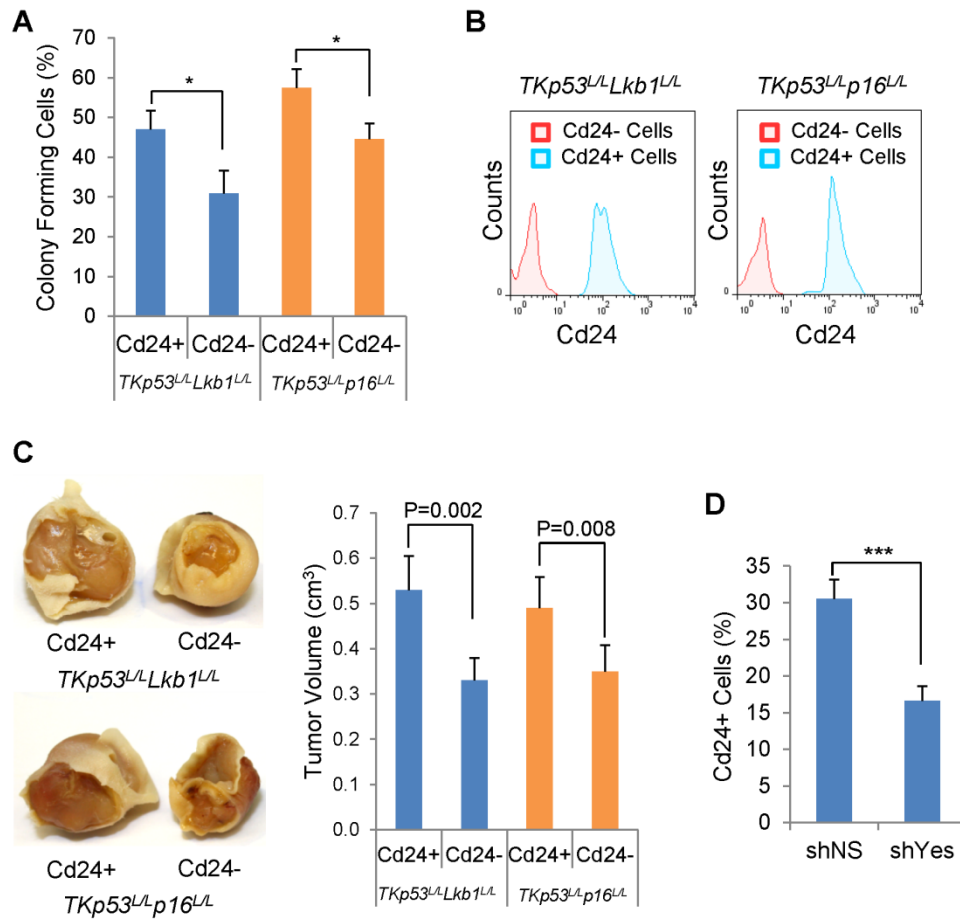


Figure S6, Microarray analysis of *Lkb1*-regulated transcripts and flow cytometry analysis of the effects of *Lkb1* loss on Cd24 expression, related to Figure 6. (A-B) Hierarchical clustering of murine primary melanomas by transcripts upregulated (A) and

downregulated (B) in Lkb1-deficient tumors and cell lines. Microarray analysis and identification of the transcript list were performed as described in the experimental procedures. Cd24 as well as Mir27 and Lef1 targets are color-coded as labeled. rep: replicate. (C) Representative flow-cytometry dot plots for Cd24 expression of *Lkb1*-null (*TKLkb1<sup>L/L</sup>* and *TKp53<sup>L/L</sup>Lkb1<sup>L/L</sup>*) and *Lkb1*-competent (*TKp53<sup>L/L</sup>p16<sup>L/L</sup>* and *TRIA*) melanoma cells. (D) Representative flow-cytometry dot plots for Cd24 expression of *TKp53<sup>L/L</sup>p16<sup>L/L</sup>* cells with nonspecific shRNAs (NS) or shRNA targeting *Lkb1* (sh-*Lkb1*). Cells transduced with NS or sh-*Lkb1* expressed GFP. (E) Representative flow-cytometry dot plots for Cd24 expression of *TKp53<sup>L/L</sup>Lkb1<sup>L/L</sup>* cells transduced with pBAGE control vector, *Lkb1*-KD or *Lkb1*. (F) Tumor cells were isolated from primary *TKLkb1<sup>L/L</sup>* and *TRIA* melanomas. Isolated tumor cells were immediately subjected to flow cytometric analysis for Cd24 expression. (G) Separation of Cd24<sup>+</sup> and Cd24<sup>-</sup> cells from *TKp53<sup>L/L</sup>Lkb1<sup>L/L</sup>* cells. (H) Growth curves of Cd24<sup>+</sup> cells and Cd24<sup>-</sup> cells isolated from *TKp53<sup>L/L</sup>Lkb1<sup>L/L</sup>* cells. Error bars show standard deviation in panels F, H. \*\*\*: p<0.001.



**Figure S7, Signaling in LKB1-deficient melanoma cells, related to Figure 7.** (A) Representative flow-cytometry dot plots for CD24 and CD44 expression of A2058 cells transduced with NS or shLKB1. NS: nonspecific shRNA. (B) Separation of CD24<sup>+</sup> and CD24<sup>-</sup> cells from A2058 cells transduced with shLKB1 by FACS. (C-D) Cell lysates were prepared from isolated CD24<sup>+</sup> and CD24<sup>-</sup> cells as indicated in panel B and from A2058 cells transduced with NS. Cell lysates were then analyzed by western blot as indicated. (E) Cd24 expression of *TKp53<sup>L/L</sup>Lkb1<sup>L/L</sup>* cells after dasatinib treatment for 72 hours.



**Figure S8, Cd24<sup>+</sup> cells show increased malignant growth compared to isogenic Cd24<sup>-</sup> cells, related to Figure 8.** (A) Colony forming efficiencies as measured by plating a single cell per well of Cd24<sup>+</sup> and Cd24<sup>-</sup> cells from Lkb1-competent and -deficient cell lines of indicated genotypes. Colony forming cells were counted for each 96-well plate. (B) Separation of Cd24<sup>+</sup> and Cd24<sup>-</sup> cells from *TKp53<sup>L/L</sup>Lkb1<sup>L/L</sup>* cells and *TKp53<sup>L/L</sup>p16<sup>L/L</sup>* cells. (C) Cd24<sup>+</sup> and Cd24<sup>-</sup> cells were isolated from Lkb1-competent and -deficient cell lines by FACS and injected into the ears of nude mice. N=5 for each group. Left shows representative images by cell line genotype, and right shows mean tumor volume. (D) *TKp53<sup>L/L</sup>Lkb1<sup>L/L</sup>* cells transduced with NS or shYes were injected into nude mice via tail vein. Three weeks later, tumor cells isolated from the *in vivo* metastasis were examined



by flow cytometry for Cd24 expression. Error bars show standard deviation in panels A, C, D. \*:  $p < 0.05$ ; \*\*\*:  $p < 0.001$ .

## **SUPPLEMENTAL EXPERIMENTAL PROCEDURES**

### **Scratch Assay Movie**

Cells were plated at 150,000 cells/well in 1 ml of media (DMEM, 10% FBS) in coated 24-well plates. 24 hours after plating, the cells were scratched once with a 200 ul pipette down the center of the plate and immediately imaged on the Olympus IX70 for 12 hours. Images were taken every 30 minutes during that 12-hour time period. During imaging, the cells were kept at 5% CO<sub>2</sub>, 20% O<sub>2</sub>.

### **Soft agar colony assay**

A total of 5000 cells were suspended in 0.35% agarose diluted in growth medium and placed on top of a 0.5% agar foundation in 6-well culture plates. Cells were then incubated in a 37°C incubator and allowed to grow for 2 to 3 weeks. The colonies were stained with 0.005% Crystal Violet and counted under a light microscope at 5x magnification. Experiments were repeated three times.

### **Cell line Array Analysis**

Melanocytes and melanoma cell lines were grown as previously described (Sambade et al., 2011). All cell lines were confirmed to be free of mycoplasma contamination using the GenProbe<sup>R</sup> kit (Gen-Probe Inc.). Cell pellets were fixed in 10% buffered formalin, processed and embedded in paraffin wax. Three 1 mm diameter cores were removed from each cell line block and randomly embedded into the CLA block. CLA block was cut into 5 micron-thick sections that were placed on positively charged glass slides. CLA sections were deparaffinized and hydrated. Antigen retrieval was performed for 30 min at 100°C in Bond-epitope retrieval solution 1 pH-6.0 (AR9961). Slides were then incubated in Bond peroxide block (DS9800) and serum-free protein block (DAKO North

America, Inc.). After incubation with LKB1 antibody, which is a novel monoclonal provided as a kind gift from Diego Castrillon at UTSW, sections were incubated with secondary antibody using the DAKO Envision+ System-HRP (rabbit), followed by Diaminobenzidine (DAB) staining. H&E and IHC stained CLA sections were digitally imaged using the Aperio ScanScope XT (Aperio Technologies). Slides were de-arrayed to visualize individual cores, using TMA Lab (Aperio). CLA digital images were stored and analyzed within the Aperio Spectrum Database. Expression of LKB1 was measured using Aperio V9 color deconvolution (area analysis) algorithms using default settings. The color deconvolution algorithm score (0-300) output was used to estimate target protein expression.

### **Microarray Analysis**

Total RNA was collected and purified from tumor and cell line samples using Qiagen's RNeasy kit, with the quantity and quality determined using a Nanodrop spectrophotometer. 2µg of total RNA was labeled with either Cy3-dye for a murine common reference sample (Herschkowitz et al., 2007) or Cy5-dye for experimental samples using Agilent's Quick-Amp labeling kit. 2µg of labeled reference and experimental cRNA were co-hybridized to a custom Agilent 4X180K whole mouse DNA microarray at 65 degrees Celsius for 17 hours (Prat et al., 2010). After washing, the microarrays were scanned using an Agilent DNA microarray scanner and the features were extracted using Agilent Feature Extraction software version 10.7.3.1. The data were uploaded to the University of North Carolina Microarray Database (UMD, <https://genome.unc.edu/pubsup/breastGEO/clinicalData.shtml>) and to the Gene Expression Omnibus (GEO) under accession number GEO: GSE34866. Gene expression data was extracted from the UMD for each sample as the log<sub>2</sub> Cy5/Cy3 ratio, filtering for probes with Lowest normalized intensity values greater than 10 in both

channels and for probes with data on greater than 70% of the microarrays (Prat et al., 2010). Each probe was median centered to obtain the final dataset (Prat et al., 2010). Hierarchical clustering was performed using Gene Cluster 3.0 (de Hoon et al., 2004) and the data was viewed using Java Treeview version 1.1.5r2 (Saldanha, 2004).

Statistically significant expression changes were determined using a 2-class paired significance analysis of microarray (SAM) analysis for cell line samples and a 2-class unpaired SAM analysis for tumor samples (Tusher et al., 2001). Gene expression of probes with a false discovery rate (FDR)  $\leq$  5% were considered to be statistically significant.

The top 1000 upregulated and downregulated genes, as ranked by the SAM score, were compared for overlap between the tumor and cell line samples. Genes that were upregulated or downregulated in both datasets (“overlap” list) were separately analyzed for categorical enrichment using the gene set enrichment analysis (GSEA) molecular signature database (MSigDB) v3.0 (Subramanian et al., 2005). All gene sets in the MSigDB were considered for enrichment. Top10 upregulated and downregulated gene sets were shown in Supplemental Table S3.

### **Xenograft Experiments**

Five to six week-old female *nu/nu* mice were maintained under pathogen-free conditions. Cells were sorted by FACS and 5,000 sorted cells were injected subcutaneously on the dorsal side of the ears as previously reported (Rozenberg et al., 2010). After three weeks, animals were sacrificed and tumor sizes were measured using calipers. Tumor volume was calculated as  $(\text{length} \times \text{width}^2) / 2$ . A two-sided Student's two-tailed t-test was applied for statistical analyses.

**Cell Migration and Invasion Assays:** The *in vitro* scratch (wound healing) assay was performed as described previously (Carretero et al., 2010). Briefly, a 1mm wide scratch was made on a confluent monolayer, and cells were then allowed to grow under standard conditions for 12 hours. The migrated distance was quantified using Image J software. The “Closure Index” shown in figures was determined as  $1-f$ , where  $f$  is calculated as the remaining gap area divided by the starting scratched area. Cell invasion was measured using matrigel invasion assay using invasion chambers obtained from BD Biosciences, with assays performed according to the manufacturer’s instructions. Cells of the indicated genotypes ( $2.5 \times 10^4$ ) were added to the upper chamber in 500 ul of serum-free medium, and the lower chamber was filled with 750 ul of medium containing 10% fetal bovine serum as an attractant. After 24 hours of incubation, cells on the underside of the filter were fixed, stained and counted. For dasatinib treatment, 30 nM dasatinib was added to both upper and lower chambers 6 hours after cells were seeded, to allow cell attachment.

**Quantitative RT-PCR:** Total RNA was purified by using RNeasy Mini Kit (Qiagen) and SuperScript<sup>®</sup> Synthesis System for RT-PCR (Invitrogen) was used to synthesize first-strand cDNA from total RNA. RT-PCR reactions were prepared in triplicate for each sample and run on 7900HT Fast Real-Time PCR System (Applied Biosystems). Taqman probe for human CD24 was purchased from Applied Biosystems. 18S (Applied Biosystems) was used as a reference for all reactions. Relative mRNA expression was determined by DDCT method.

**Src 8-plex analysis:** Quantification of Src family kinase activities were assayed using SRC Family Kinase 8-Plex (Millipore). Assays were performed according to the

manufacturer's specifications and analyzed with a Luminex 200 platform. Briefly, 20mg of protein per sample was incubated with Luminex beads conjugated with SFK (Src family kinases) specific antibody. Following the incubation, the beads were washed and incubated with biotinylated antibody targeting tyrosine 419 on an active loop. The bead conjugates were then washed and incubated with phycoerythrin. Mean fluorescence intensity (MFI) from duplicate samples was averaged with background correction from duplicate samples. Statistical significance was calculated using a two-sided Student's exact t-test.

**Immunoprecipitation, Immunoblotting and Immunofluorescence:** Cell lysates were prepared in RIPA buffer with protease inhibitors (Roche, Indianapolis, IN, USA) and phosphatase inhibitors (Calbiochem, EMD Chemicals Inc, Darmstadt, Germany). For immunoprecipitation, cell lysates were precleared with Protein A/G agarose beads for 1 hour, incubated with indicated antibody overnight at 4°C, mixed with Protein A/G agarose beads, incubated for 3 hours, and then washed with lysis buffer five times. The immunoprecipitates were then subjected to immunoblotting.

For immunoblotting, standard western blot procedures were performed after resolution on polyacrylamide gels. Antibodies used were  $\beta$ -Actin (Santa Cruz), LKB1 (Cell Signaling), SRC (Cell Signaling), FYN (Santa Cruz), YES (Santa Cruz), p-SFK (Tyr416, Cell Signaling), p-ERK1/2 (Cell Signaling), ERK1/2 (Cell Signaling), p-AKT (Cell Signaling), AKT (Cell Signaling), p16<sup>Ink4a</sup> (Santa Cruz), p19<sup>Arf</sup> (Abcam). Band intensity was quantified using a LiCor Odyssey<sup>®</sup> Infrared Imaging System.

For immunofluorescence, cells were grown on coverslips. After fixation in 4% paraformaldehyde, cells were permeabilized in 0.1% Triton X-100, blocked in 10%

normal goat serum and incubated with indicated primary antibody for 1 hour. Cells were washed three times and then incubated with an Alexa Fluor 488-conjugated secondary anti-rabbit antibody for 45 minutes.

## REFERENCES TO SUPPLEMENTARY MATERIAL:

Carretero, J., Shimamura, T., Rikova, K., Jackson, A. L., Wilkerson, M. D., Borgman, C. L., Buttarazzi, M. S., Sanofsky, B. A., McNamara, K. L., Brandstetter, K. A., *et al.* (2010). Integrative genomic and proteomic analyses identify targets for Lkb1-deficient metastatic lung tumors. *Cancer Cell* 17, 547-559.

de Hoon, M. J., Imoto, S., Nolan, J., and Miyano, S. (2004). Open source clustering software. *Bioinformatics* 20, 1453-1454.

Herschkowitz, J. I., Simin, K., Weigman, V. J., Mikaelian, I., Usary, J., Hu, Z., Rasmussen, K. E., Jones, L. P., Assefnia, S., Chandrasekharan, S., *et al.* (2007). Identification of conserved gene expression features between murine mammary carcinoma models and human breast tumors. *Genome Biol* 8, R76.

Prat, A., Parker, J. S., Karginova, O., Fan, C., Livasy, C., Herschkowitz, J. I., He, X., and Perou, C. M. (2010). Phenotypic and molecular characterization of the claudin-low intrinsic subtype of breast cancer. *Breast Cancer Res* 12, R68.

Rozenberg, G. I., Monahan, K. B., Torrice, C., Bear, J. E., and Sharpless, N. E. (2010). Metastasis in an orthotopic murine model of melanoma is independent of RAS/RAF mutation. *Melanoma Res* 20, 361-371.

Saldanha, A. J. (2004). Java Treeview--extensible visualization of microarray data. *Bioinformatics* 20, 3246-3248.

Sambade, M. J., Peters, E. C., Thomas, N. E., Kaufmann, W. K., Kimple, R. J., and Shields, J. M. (2011). Melanoma cells show a heterogeneous range of sensitivity to ionizing radiation and are radiosensitized by inhibition of B-RAF with PLX-4032. *Radiother Oncol* 98, 394-399.

Subramanian, A., Tamayo, P., Mootha, V. K., Mukherjee, S., Ebert, B. L., Gillette, M. A., Paulovich, A., Pomeroy, S. L., Golub, T. R., Lander, E. S., and Mesirov, J. P. (2005). Gene set enrichment analysis: a knowledge-based approach for interpreting genome-wide expression profiles. *Proc Natl Acad Sci U S A* 102, 15545-15550.

Tusher, V. G., Tibshirani, R., and Chu, G. (2001). Significance analysis of microarrays applied to the ionizing radiation response. *Proc Natl Acad Sci U S A* 98, 5116-5121.